

Measurement of the Cross Section for Prompt Isolated Diphoton Production in $p\bar{p}$ Collisions at $\sqrt{s} = 1.96$ TeV

T. Aaltonen,²¹ B. Álvarez González,^{9,v} S. Amerio,^{41a} D. Amidei,³² A. Anastassov,³⁶ A. Annovi,¹⁷ J. Antos,¹² G. Apollinari,¹⁵ J. A. Appel,¹⁵ A. Apresyan,⁴⁶ T. Arisawa,⁵⁶ A. Artikov,¹³ J. Asaadi,⁵¹ W. Ashmanskas,¹⁵ B. Auerbach,⁵⁹ A. Aurisano,⁵¹ F. Azfar,⁴⁰ W. Badgett,¹⁵ A. Barbaro-Galtieri,²⁶ V. E. Barnes,⁴⁶ B. A. Barnett,²³ P. Barria,^{44c,44a} P. Bartos,¹² M. Baucé,^{41b,41a} G. Bauer,³⁰ F. Bedeschi,^{44a} D. Beecher,²⁸ S. Behari,²³ G. Bellettini,^{44b,44a} J. Bellinger,⁵⁸ D. Benjamin,¹⁴ A. Beretvas,¹⁵ A. Bhatti,⁴⁸ M. Binkley,^{15a} D. Bisello,^{41b,41a} I. Bizjak,^{28,z} K. R. Bland,⁵ B. Blumenfeld,²³ A. Bocci,¹⁴ A. Bodek,⁴⁷ D. Bortoletto,⁴⁶ J. Boudreau,⁴⁵ A. Boveia,¹¹ B. Brau,^{15,b} L. Brigliadori,^{6b,6a} A. Brisuda,¹² C. Bromberg,³³ E. Brucken,²¹ M. Bucciantonio,^{44b,44a} J. Budagov,¹³ H. S. Budd,⁴⁷ S. Budd,²² K. Burkett,¹⁵ G. Busetto,^{41b,41a} P. Bussey,¹⁹ A. Buzatu,³¹ C. Calancha,²⁹ S. Camarda,⁴ M. Campanelli,³³ M. Campbell,³² F. Canelli,^{12,15} A. Canepa,⁴³ B. Carls,²² D. Carlsmith,⁵⁸ R. Carosi,^{44a} S. Carrillo,^{16,l} S. Carron,¹⁵ B. Casal,⁹ M. Casarsa,¹⁵ A. Castro,^{6b,6a} P. Catastini,¹⁵ D. Cauz,^{52a} V. Cavaliere,^{44c,44a} M. Cavalli-Sforza,⁴ A. Cerri,^{26,g} L. Cerrito,^{28,q} Y. C. Chen,¹ M. Chertok,⁷ G. Chiarelli,^{44a} G. Chlachidze,¹⁵ F. Chlebana,¹⁵ K. Cho,²⁵ D. Chokheli,¹³ J. P. Chou,²⁰ W. H. Chung,⁵⁸ Y. S. Chung,⁴⁷ C. I. Ciobanu,⁴² M. A. Ciocci,^{44c,44a} A. Clark,¹⁸ G. Compostella,^{41b,41a} M. E. Convery,¹⁵ J. Conway,⁷ M. Corbo,⁴² M. Cordelli,¹⁷ C. A. Cox,⁷ D. J. Cox,⁷ F. Crescioli,^{44b,44a} C. Cuenca Almenar,⁵⁹ J. Cuevas,^{9,v} R. Culbertson,¹⁵ D. Dagenhart,¹⁵ N. d'Ascenzo,^{42,t} M. Datta,¹⁵ P. de Barbaro,⁴⁷ S. De Cecco,^{49a} G. De Lorenzo,⁴ M. Dell'Orso,^{44b,44a} C. Deluca,⁴ L. Demortier,⁴⁸ J. Deng,^{14,d} M. Deninno,^{6a} F. Devoto,²¹ M. d'Errico,^{41b,41a} A. Di Canto,^{44b,44a} B. Di Ruzza,^{44a} J. R. Dittmann,⁵ M. D'Onofrio,²⁷ S. Donati,^{44b,44a} P. Dong,¹⁵ M. Dorigo,^{52a} T. Dorigo,^{41a} K. Ebina,⁵⁶ A. Elagin,⁵¹ A. Eppig,³² R. Erbacher,⁷ D. Errede,²² S. Errede,²² N. Ershaidat,^{42,y} R. Eusebi,⁵¹ H. C. Fang,²⁶ S. Farrington,⁴⁰ M. Feindt,²⁴ J. P. Fernandez,²⁹ C. Ferrazza,^{44d,44a} R. Field,¹⁶ G. Flanagan,^{46,r} R. Forrest,⁷ M. J. Frank,⁵ M. Franklin,²⁰ J. C. Freeman,¹⁵ Y. Funakoshi,⁵⁶ I. Furic,¹⁶ M. Gallinaro,⁴⁸ J. Galyardt,¹⁰ J. E. Garcia,¹⁸ A. F. Garfinkel,⁴⁶ P. Garosi,^{44c,44a} H. Gerberich,²² E. Gerchtein,¹⁵ S. Giagu,^{49b,49a} V. Giakoumopoulou,³ P. Giannetti,^{44a} K. Gibson,⁴⁵ C. M. Ginsburg,¹⁵ N. Giokaris,³ P. Giromini,¹⁷ M. Giunta,^{44a} G. Giurgiu,²³ V. Glagolev,¹³ D. Glenzinski,¹⁵ M. Gold,³⁵ D. Goldin,⁵¹ N. Goldschmidt,¹⁶ A. Golossanov,¹⁵ G. Gomez,⁹ G. Gomez-Ceballos,³⁰ M. Goncharov,³⁰ O. González,²⁹ I. Gorelov,³⁵ A. T. Goshaw,¹⁴ K. Goulianos,⁴⁸ A. Gresele,^{41a} S. Grinstein,⁴ C. Grosso-Pilcher,¹¹ R. C. Group,⁵⁵ J. Guimaraes da Costa,²⁰ Z. Gunay-Unalan,³³ C. Haber,²⁶ S. R. Hahn,¹⁵ E. Halkiadakis,⁵⁰ A. Hamaguchi,³⁹ J. Y. Han,⁴⁷ F. Happacher,¹⁷ K. Hara,⁵³ D. Hare,⁵⁰ M. Hare,⁵⁴ R. F. Harr,⁵⁷ K. Hatakeyama,⁵ C. Hays,⁴⁰ M. Heck,²⁴ J. Heinrich,⁴³ M. Herndon,⁵⁸ S. Hewamanage,⁵ D. Hidas,⁵⁰ A. Hocker,¹⁵ W. Hopkins,^{15,h} D. Horn,²⁴ S. Hou,¹ R. E. Hughes,³⁷ M. Hurwitz,¹¹ U. Husemann,⁵⁹ N. Hussain,³¹ M. Hussein,³³ J. Huston,³³ G. Introzzi,^{44a} M. Iori,^{49b,49a} A. Ivanov,^{7,o} E. James,¹⁵ D. Jang,¹⁰ B. Jayatilaka,¹⁴ E. J. Jeon,²⁵ M. K. Jha,^{6a} S. Jindariani,¹⁵ W. Johnson,⁷ M. Jones,⁴⁶ K. K. Joo,²⁵ S. Y. Jun,¹⁰ T. R. Junk,¹⁵ T. Kamon,⁵¹ P. E. Karchin,⁵⁷ Y. Kato,^{39,b} W. Ketchum,¹¹ J. Keung,⁴³ V. Khotilovich,⁵¹ B. Kilminster,¹⁵ D. H. Kim,²⁵ H. S. Kim,²⁵ H. W. Kim,²⁵ J. E. Kim,²⁵ M. J. Kim,¹⁷ S. B. Kim,²⁵ S. H. Kim,⁵³ Y. K. Kim,¹¹ N. Kimura,⁵⁶ M. Kirby,¹⁵ S. Klimenko,¹⁶ K. Kondo,⁵⁶ D. J. Kong,²⁵ J. Konigsberg,¹⁶ A. V. Kotwal,¹⁴ M. Kreps,²⁴ J. Kroll,⁴³ D. Krop,¹¹ N. Krumnack,^{5,m} M. Kruse,¹⁴ V. Krutelyov,^{51,e} T. Kuhr,²⁴ M. Kurata,⁵³ S. Kwang,¹¹ A. T. Laasanen,⁴⁶ S. Lami,^{44a} S. Lammel,¹⁵ M. Lancaster,²⁸ R. L. Lander,⁷ K. Lannon,^{37,u} A. Lath,⁵⁰ G. Latino,^{44a,d} I. Lazzizzera,^{41a} T. LeCompte,² E. Lee,⁵¹ H. S. Lee,¹¹ J. S. Lee,²⁵ S. W. Lee,^{51,w} S. Leo,^{44b,44a} S. Leone,^{44a} J. D. Lewis,¹⁵ C.-J. Lin,²⁶ J. Linacre,⁴⁰ M. Lindgren,¹⁵ E. Lipeles,⁴³ A. Lister,¹⁸ D. O. Litvintsev,¹⁵ C. Liu,⁴⁵ Q. Liu,⁴⁶ T. Liu,¹⁵ S. Lockwitz,⁵⁹ N. S. Lockyer,⁴³ A. Loginov,⁵⁹ D. Lucchesi,^{41b,41a} J. Lueck,²⁴ P. Lujan,²⁶ P. Lukens,¹⁵ G. Lungu,⁴⁸ J. Lys,²⁶ R. Lysak,¹² R. Madrak,¹⁵ K. Maeshima,¹⁵ K. Makhoul,³⁰ P. Maksimovic,²³ S. Malik,⁴⁸ G. Manca,^{27,c} A. Manousakis-Katsikakis,³ F. Margaroli,⁴⁶ C. Marino,²⁴ M. Martínez,⁴ R. Martínez-Ballarín,²⁹ P. Mastrandrea,^{49a} M. Mathis,²³ M. E. Mattson,⁵⁷ P. Mazzanti,^{6a} K. S. McFarland,⁴⁷ P. McIntyre,⁵¹ R. McNulty,^{27,j} A. Mehta,²⁷ P. Mehtala,²¹ A. Menzione,^{44a} C. Mesropian,⁴⁸ T. Miao,¹⁵ D. Mietlicki,³² A. Mitra,¹ H. Miyake,⁵³ S. Moed,²⁰ N. Moggi,^{6a} M. N. Mondragon,^{15,l} C. S. Moon,²⁵ R. Moore,¹⁵ M. J. Morello,¹⁵ J. Morlock,²⁴ P. Movilla Fernandez,¹⁵ A. Mukherjee,¹⁵ Th. Muller,²⁴ P. Murat,¹⁵ M. Mussini,^{6b,6a} J. Nachtman,^{15,n} Y. Nagai,⁵³ J. Naganoma,⁵⁶ I. Nakano,³⁸ A. Napier,⁵⁴ J. Nett,⁵¹ C. Neu,⁵⁵ M. S. Neubauer,²² J. Nielsen,^{26,f} L. Nodulman,² O. Norniella,²² E. Nurse,²⁸ L. Oakes,⁴⁰ S. H. Oh,¹⁴ Y. D. Oh,²⁵ I. Oksuzian,⁵⁵ T. Okusawa,³⁹ R. Orava,²¹ L. Ortolan,⁴ S. Pagan Griso,^{41b,41a} C. Pagliarone,^{52a} E. Palencia,^{9,g} V. Papadimitriou,¹⁵ A. A. Paramonov,² J. Patrick,¹⁵ G. Pauletta,^{52a,g} M. Paulini,¹⁰ C. Paus,³⁰ D. E. Pellett,⁷ A. Penzo,^{52a} T. J. Phillips,¹⁴ G. Piacentino,^{44a} E. Pianori,⁴³ J. Pilot,³⁷ K. Pitts,²² C. Plager,⁸ L. Pondrom,⁵⁸ K. Potamianos,⁴⁶ O. Poukhov,^{13,a} A. Pranko,⁶⁰ F. Prokoshin,^{13,x} F. Ptohos,^{17,i} E. Pueschel,¹⁰ G. Punzi,^{44b,44a} J. Pursley,⁵⁸ A. Rahaman,⁴⁵ V. Ramakrishnan,⁵⁸ N. Ranjan,⁴⁶ I. Redondo,²⁹ P. Renton,⁴⁰ M. Rescigno,^{49a}

F. Rimondi,^{6b,6a} L. Ristori,^{44a,15} A. Robson,¹⁹ T. Rodrigo,⁹ T. Rodriguez,⁴³ E. Rogers,²² S. Rolli,⁵⁴ R. Roser,¹⁵ M. Rossi,^{52a}
 F. Rubbo,¹⁵ F. Ruffini,^{44c,44a} A. Ruiz,⁹ J. Russ,¹⁰ V. Rusu,¹⁵ A. Safonov,⁵¹ W. K. Sakumoto,⁴⁷ Y. Sakurai,⁵⁶ L. Santi,^{52b,52a}
 L. Sartori,^{44a} K. Sato,⁵³ V. Saveliev,^{42,t} A. Savoy-Navarro,⁴² P. Schlabach,¹⁵ A. Schmidt,²⁴ E. E. Schmidt,¹⁵
 M. P. Schmidt,^{59,a} M. Schmitt,³⁶ T. Schwarz,⁷ L. Scodellaro,⁹ A. Scribano,^{44c,44a} F. Scuri,^{44a} A. Sedov,⁴⁶ S. Seidel,³⁵
 Y. Seiya,³⁹ A. Semenov,¹³ F. Sforza,^{44b,44a} A. Sfyrta,²² D. Sgalaberna,^{6b} S. Z. Shalhout,⁷ T. Shears,²⁷ P. F. Shepard,⁴⁵
 M. Shimojima,^{53,s} S. Shiraishi,¹¹ M. Shochet,¹¹ I. Shreyber,³⁴ A. Simonenko,¹³ P. Sinervo,³¹ A. Sissakian,^{13,a} K. Sliwa,⁵⁴
 J. R. Smith,⁷ F. D. Snider,¹⁵ A. Soha,¹⁵ S. Somalwar,⁵⁰ V. Sorin,⁴ P. Squillacioti,¹⁵ M. Stancari,¹⁵ M. Stanitzki,⁵⁹
 R. St. Denis,¹⁹ B. Stelzer,³¹ O. Stelzer-Chilton,³¹ D. Stentz,³⁶ J. Strologas,³⁵ G. L. Strycker,³² Y. Sudo,⁵³ A. Sukhanov,¹⁶
 I. Suslov,¹³ K. Takemasa,⁵³ Y. Takeuchi,⁵³ J. Tang,¹¹ M. Tecchio,³² P. K. Teng,¹ J. Thom,^{15,h} J. Thome,¹⁰
 G. A. Thompson,²² E. Thomson,⁴³ P. Ttito-Guzmán,²⁹ S. Tkaczyk,¹⁵ D. Toback,⁵¹ S. Tokar,¹² K. Tollefson,³³ T. Tomura,⁵³
 D. Tonelli,¹⁵ S. Torre,¹⁷ D. Torretta,¹⁵ P. Totaro,^{52b,52a} M. Trovato,^{44d,44a} Y. Tu,⁴³ F. Ukegawa,⁵³ S. Uozumi,²⁵
 A. Varganov,³² F. Vázquez,^{16,l} G. Velev,¹⁵ C. Vellidis,³ M. Vidal,²⁹ I. Vila,⁹ R. Vilar,⁹ J. Vizán,⁹ M. Vogel,³⁵ G. Volpi,^{44b,44a}
 P. Wagner,⁴³ R. L. Wagner,¹⁵ T. Wakisaka,³⁹ R. Wallny,⁸ S. M. Wang,¹ A. Warburton,³¹ D. Waters,²⁸ M. Weinberger,⁵¹
 W. C. Wester III,¹⁵ B. Whitehouse,⁵⁴ D. Whiteson,^{43,d} A. B. Wicklund,² E. Wicklund,¹⁵ S. Wilbur,¹¹ F. Wick,²⁴
 H. H. Williams,⁴³ J. S. Wilson,³⁷ P. Wilson,¹⁵ B. L. Winer,³⁷ P. Wittich,^{15,h} S. Wolbers,¹⁵ H. Wolfe,³⁷ T. Wright,³² X. Wu,¹⁸
 Z. Wu,⁵ K. Yamamoto,³⁹ J. Yamaoka,¹⁴ T. Yang,¹⁵ U. K. Yang,^{11,p} Y. C. Yang,²⁵ W.-M. Yao,²⁶ G. P. Yeh,¹⁵ K. Yi,^{15,n}
 J. Yoh,¹⁵ K. Yorita,⁵⁶ T. Yoshida,^{39,k} G. B. Yu,¹⁴ I. Yu,²⁵ S. S. Yu,¹⁵ J. C. Yun,¹⁵ A. Zanetti,^{52a}
 Y. Zeng,¹⁴ and S. Zucchelli^{6b,6a}

(CDF Collaboration)

¹*Institute of Physics, Academia Sinica, Taipei, Taiwan 11529, Republic of China*²*Argonne National Laboratory, Argonne, Illinois 60439, USA*³*University of Athens, 157 71 Athens, Greece*⁴*Institut de Física d'Altes Energies, ICREA, Universitat Autònoma de Barcelona, E-08193, Bellaterra (Barcelona), Spain*⁵*Baylor University, Waco, Texas 76798, USA*^{6a}*Istituto Nazionale di Fisica Nucleare Bologna, I-40127 Bologna, Italy*^{6b}*University of Bologna, I-40127 Bologna, Italy*⁷*University of California, Davis, Davis, California 95616, USA*⁸*University of California, Los Angeles, Los Angeles, California 90024, USA*⁹*Instituto de Física de Cantabria, CSIC-University of Cantabria, 39005 Santander, Spain*¹⁰*Carnegie Mellon University, Pittsburgh, Pennsylvania 15213, USA*¹¹*Enrico Fermi Institute, University of Chicago, Chicago, Illinois 60637, USA*¹²*Comenius University, 842 48 Bratislava, Slovakia; Institute of Experimental Physics, 040 01 Kosice, Slovakia*¹³*Joint Institute for Nuclear Research, RU-141980 Dubna, Russia*¹⁴*Duke University, Durham, North Carolina 27708, USA*¹⁵*Fermi National Accelerator Laboratory, Batavia, Illinois 60510, USA*¹⁶*University of Florida, Gainesville, Florida 32611, USA*¹⁷*Laboratori Nazionali di Frascati, Istituto Nazionale di Fisica Nucleare, I-00044 Frascati, Italy*¹⁸*University of Geneva, CH-1211 Geneva 4, Switzerland*¹⁹*Glasgow University, Glasgow G12 8QQ, United Kingdom*²⁰*Harvard University, Cambridge, Massachusetts 02138, USA*²¹*Division of High Energy Physics, Department of Physics, University of Helsinki and Helsinki Institute of Physics, FIN-00014, Helsinki, Finland*²²*University of Illinois, Urbana, Illinois 61801, USA*²³*The Johns Hopkins University, Baltimore, Maryland 21218, USA*²⁴*Institut für Experimentelle Kernphysik, Karlsruhe Institute of Technology, D-76131 Karlsruhe, Germany*²⁵*Center for High Energy Physics: Kyungpook National University, Daegu 702-701, Korea; Seoul National University, Seoul 151-742, Korea; Sungkyunkwan University, Suwon 440-746, Korea; Korea Institute of Science and Technology Information, Daejeon 305-806, Korea; Chonnam National University, Gwangju 500-757, Korea; Chonbuk National University, Jeonju 561-756, Korea*²⁶*Ernest Orlando Lawrence Berkeley National Laboratory, Berkeley, California 94720, USA*²⁷*University of Liverpool, Liverpool L69 7ZE, United Kingdom*²⁸*University College London, London WC1E 6BT, United Kingdom*²⁹*Centro de Investigaciones Energéticas Medioambientales y Tecnológicas, E-28040 Madrid, Spain*³⁰*Massachusetts Institute of Technology, Cambridge, Massachusetts 02139, USA*

- ³¹*Institute of Particle Physics: McGill University, Montréal, Québec, Canada H3A 2T8; Simon Fraser University, Burnaby, British Columbia, Canada V5A 1S6; University of Toronto, Toronto, Ontario, Canada M5S 1A7; and TRIUMF, Vancouver, British Columbia, Canada V6T 2A3*
- ³²*University of Michigan, Ann Arbor, Michigan 48109, USA*
- ³³*Michigan State University, East Lansing, Michigan 48824, USA*
- ³⁴*Institution for Theoretical and Experimental Physics, ITEP, Moscow 117259, Russia*
- ³⁵*University of New Mexico, Albuquerque, New Mexico 87131, USA*
- ³⁶*Northwestern University, Evanston, Illinois 60208, USA*
- ³⁷*The Ohio State University, Columbus, Ohio 43210, USA*
- ³⁸*Okayama University, Okayama 700-8530, Japan*
- ³⁹*Osaka City University, Osaka 588, Japan*
- ⁴⁰*University of Oxford, Oxford OX1 3RH, United Kingdom*
- ^{41a}*Istituto Nazionale di Fisica Nucleare, Sezione di Padova-Trento, I-35131 Padova, Italy*
- ^{41b}*University of Padova, I-35131 Padova, Italy*
- ⁴²*LPNHE, USA Université Pierre et Marie Curie/IN2P3-CNRS, UMR7585, Paris, F-75252 France*
- ⁴³*University of Pennsylvania, Philadelphia, Pennsylvania 19104, USA*
- ^{44a}*Istituto Nazionale di Fisica Nucleare Pisa, I-56127 Pisa, Italy*
- ^{44b}*University of Pisa, I-56127 Pisa, Italy*
- ^{44c}*University of Siena, I-56127 Pisa, Italy*
- ^{44d}*Scuola Normale Superiore, I-56127 Pisa, Italy*
- ⁴⁵*University of Pittsburgh, Pittsburgh, Pennsylvania 15260, USA*
- ⁴⁶*Purdue University, West Lafayette, Indiana 47907, USA*
- ⁴⁷*University of Rochester, Rochester, New York 14627, USA*
- ⁴⁸*The Rockefeller University, New York, New York 10065, USA*
- ^{49a}*Istituto Nazionale di Fisica Nucleare, Sezione di Roma 1, I-00185 Roma, Italy*
- ^{49b}*Sapienza Università di Roma, I-00185 Roma, Italy*
- ⁵⁰*Rutgers University, Piscataway, New Jersey 08855, USA*
- ⁵¹*Texas A&M University, College Station, Texas 77843, USA*
- ^{52a}*Istituto Nazionale di Fisica Nucleare Trieste/Udine, I-34100 Trieste, Italy*
- ^{52b}*University of Trieste/Udine, I-33100 Udine, Italy*
- ⁵³*University of Tsukuba, Tsukuba, Ibaraki 305, Japan*
- ⁵⁴*Tufts University, Medford, Massachusetts 02155, USA*
- ⁵⁵*University of Virginia, Charlottesville, Virginia 22906, USA*
- ⁵⁶*Waseda University, Tokyo 169, Japan*
- ⁵⁷*Wayne State University, Detroit, Michigan 48201, USA*
- ⁵⁸*University of Wisconsin, Madison, Wisconsin 53706, USA*
- ⁵⁹*Yale University, New Haven, Connecticut 06520, USA*
- ⁶⁰*Ernest Orlando Lawrence Berkeley National Laboratory, Berkeley, California 94720, USA*

(Received 29 June 2011; published 2 September 2011)

This Letter reports a measurement of the cross section of prompt isolated photon pair production in $p\bar{p}$ collisions at a total energy $\sqrt{s} = 1.96$ TeV using data of 5.36 fb^{-1} integrated luminosity collected with the CDF II detector at the Fermilab Tevatron. The measured cross section, differential in basic kinematic variables, is compared with three perturbative QCD predictions, a leading order parton shower calculation and two next-to-leading order calculations. The next-to-leading order calculations reproduce most aspects of the data. By including photon radiation from quarks before and after hard scattering, the parton shower prediction becomes competitive with the next-to-leading order predictions.

DOI: 10.1103/PhysRevLett.107.102003

PACS numbers: 13.85.Qk

The production of prompt photon pairs with large invariant mass in hadron collisions is a large irreducible background in searches for a low mass Higgs boson decaying into a photon pair [1], as well as in searches for new phenomena, such as new heavy resonances [2], extra spatial dimensions [3,4], or cascade decays of heavy new particles [5]. Precise measurements of the diphoton production differential cross sections for various kinematic variables and their theoretical understanding are thus very

important for these searches. Diphoton production is also used to check the validity of perturbative quantum chromodynamics and soft-gluon resummation methods implemented in theoretical calculations. Diphotons are expected to be dominantly produced by quark-antiquark annihilation $q\bar{q} \rightarrow \gamma\gamma$ and also in kinematic regions with high gluon luminosity, especially at low invariant mass, by gluon-gluon fusion $gg \rightarrow \gamma\gamma$ through a quark loop diagram. Prompt photons may also result from quark fragmentations

in hard scattering, although a strict photon isolation requirement significantly reduces the fragmentation contributions.

Diphoton measurements have been previously conducted at fixed-target [6] and collider experiments [7–10]. The most recent measurements [9,10] were compared with the same perturbative quantum chromodynamics calculations examined in the present work, and large discrepancies were found between the data and a LO matrix element calculation supplemented with a parton shower model, suitable for simulation of the backgrounds in searches of a low mass Higgs boson and of new phenomena. This work shows that the inclusion of photons radiated from initial and final state quarks drastically improves the comparison of the parton shower calculation with the data.

The reported measurement was conducted by using data of total integrated luminosity 5.36 fb^{-1} collected with the Collider Detector at Fermilab (CDF) [11] at the Tevatron $p\bar{p}$ collider. CDF is composed of a central spectrometer inside a 1.4 T magnetic field, surrounded by electromagnetic and hadronic calorimeters and muon detection chambers. The inner spectrometer measures charged particle tracks with a transverse momentum (p_T) precision of $\Delta p_T/p_T^2 = 0.07\%(\text{GeV}/c)^{-1}$. The central calorimeters cover the region $|\eta| < 1.1$, with an electromagnetic (hadronic) energy resolution of $\sigma(E_T)/E_T = 13.5\%/\sqrt{E_T(\text{GeV})} \oplus 1.5\%$ [$\sigma(E_T)/E_T = 50\%/\sqrt{E_T(\text{GeV})} \oplus 3\%$] and a tower segmentation of $\Delta\eta \times \Delta\phi \approx 0.1 \times 15^\circ$. Photons are reconstructed in clusters of up to three towers [12]. χ^2 criteria are imposed on the profile of the shower to match expected patterns. Two main cuts are applied: (i) The photon transverse energy is required to be $E_T \geq 17 \text{ GeV}$ for the first photon in the event and $E_T \geq 15 \text{ GeV}$ for the second photon; (ii) the calorimeter isolation energy in the isolation cone around each photon [13] is required to be less than 2 GeV.

The background from $\gamma + \text{jet}$ and dijet events, where one or two jets are faking a photon, is subtracted with a method using the track isolation as the discriminant between signal and background [14]. It is based on the substantial difference of the track isolation distribution for signal photons (nearly exponential) and for background photons (nearly flat). The advantages of this method are that (i) it has little sensitivity to multiple interactions in the colliding beams, so that the signal-background separation does not degrade at high instantaneous luminosity, and (ii) it has high efficiency and good track momentum resolution, implying minimal degradation of the signal-background separation due to instrumental effects. The signal fraction is determined by summing the probabilities of an event to be pure signal, pure background, or a mixed photon pair. These probabilities are obtained by solving a 4×4 matrix equation using the observation value (0 or 1) for all four combinations of the leading or subleading photon having track isolation below or above 1 GeV/c

as an input. The matrix is constructed from the E_T -dependent efficiencies of signal and background photons passing the track isolation cut. A threshold cut of 1 GeV/c is determined by maximizing the separation between signal and background. The efficiencies are determined from Monte Carlo (MC) $\gamma + \text{jet}$ and dijet samples, which are produced by using the PYTHIA event generator [15]. PYTHIA events are fully simulated through the detector and trigger and are reconstructed with the CDF II simulation and reconstruction software [16]. With this matrix technique the full correlations between the two photons in the event are properly taken into account. Tests are made for underlying event contributions in complementary cones to the photon reconstruction cone [17] and also using isolated tracks in dijet events. The systematic uncertainty in the signal fraction with this method is of the order of 15%–20%.

The diphoton production cross section differential in a kinematic variable is obtained from the histogram of the estimated signal in the selected variable. The average cross section in a bin of the variable is determined by dividing the bin content by the trigger efficiency, the diphoton selection efficiency and acceptance, the integrated luminosity, and the bin size. The diphoton trigger efficiency is derived from data [1]. It is consistent with 100% over all of the kinematic range with a flat uncertainty of 3%. The selection efficiency is determined from data and MC simulation with an iterative method. In the first pass the efficiency is determined from a fully simulated and reconstructed PYTHIA diphoton MC sample by dividing the number of events passing all selection cuts by the number of events passing only the kinematic cuts on the photon E_T , η , angular separation, and isolation at the event generation level. The efficiency denominator is corrected for the “underlying event” from collision remnants which make the efficiency obtained from PYTHIA too high by removing events from the denominator through the isolation cut. This correction is derived by running PYTHIA with and without underlying event and amounts to a constant factor of 0.88 per event. A flat 6% uncertainty in the selection efficiency (3% per photon) accounts for possible inaccuracies in the PYTHIA model for the underlying event. The signal events of the data are corrected for the preliminary efficiency. The data are then used to reweight the PYTHIA events and obtain a more accurate representation of the true diphoton distribution. The efficiency is determined by using the reweighted PYTHIA sample and corrected for luminosity dependence, derived from a comparison of the vertex multiplicity distribution in data and PYTHIA MC $Z^0 \rightarrow e^+e^-$ events. The systematic uncertainty in the efficiency resulting from the luminosity-dependent correction grows linearly from 1.8% for $E_T \leq 40 \text{ GeV}$ to 3% at $E_T = 80 \text{ GeV}$ and remains constant above this point. Finally, a 6% constant uncertainty comes from the Tevatron integrated luminosity [18].

The $Z^0 \rightarrow e^+e^-$ sample is used for calibration by applying a “diphotonlike” event selection, i.e., by imposing a diphoton selection with the same trigger but allowing for a track associated with each of the two electromagnetic objects in the event. The electromagnetic energy scale in data and MC simulation is corrected by tuning the $Z^0 \rightarrow e^+e^-$ mass peak to the world average [19], and a systematic uncertainty from this correction is estimated to grow linearly from 0 at $E_T \leq 40$ GeV up to 1.5% at $E_T = 80$ GeV and remain constant above this point. The difference in the photon identification efficiency between data and MC simulation is estimated from the $Z^0 \rightarrow e^+e^-$ sample [1] and added as a systematic uncertainty to the measurement. All systematic uncertainties in the cross section measurement are added in quadrature.

The results of this measurement are compared with three theoretical calculations: (i) the fixed next-to-leading order (NLO) predictions of the DIPHOX program [20] including parton fragmentations into photons [21], (ii) the predictions of the RESBOS program [22], where the cross section is accurate to NLO but also has an analytical initial state soft-gluon resummation, and (iii) the predictions of the PYTHIA program [15], which features a realistic representation of the physics events by including parton showering, initial (ISR) and final state radiation (FSR), and an underlying event model. Diphoton events were selected from an inclusive $\gamma + X$ PYTHIA sample ($X = \gamma$ or jet), thus including the $q\bar{q} \rightarrow \gamma\gamma$ and $gg \rightarrow \gamma\gamma$ processes (56%) as well as the $q\bar{q} \rightarrow g\gamma\gamma_{\text{ISR}}$, $gq \rightarrow q\gamma\gamma_{\text{ISR}}$, and $gq \rightarrow q\gamma\gamma_{\text{FSR}}$ processes (44%). This type of calculation effectively resums the cross section for gluon and photon radiation in both the initial and the final state. All calculations are subject to the experimental kinematic and isolation cuts. DIPHOX accounts for the $gg \rightarrow \gamma\gamma$ process in LO only. The predictions of RESBOS are restricted to the invariant mass range from $2m_b = 9$ GeV/ c^2 to $2m_t = 350$ GeV/ c^2 , where m_b and m_t are the masses of the bottom and top quarks, respectively. NLO theoretical uncertainties are estimated by varying the fragmentation (in DIPHOX only), renormalization, and factorization scales up and down by a factor of 2 relative to the default scale $\mu = M/2$ of DIPHOX and $\mu = M$ of RESBOS and for the NLO parton distribution function uncertainties (in both DIPHOX and RESBOS) by using the 20 CTEQ6.1M eigenvectors [23].

Figure 1 shows the comparison between the measured and predicted diphoton distributions: the diphoton invariant mass M , the diphoton transverse momentum P_T , and the difference $\Delta\phi$ between the azimuthal angles of the two photons in the event. While the PYTHIA direct calculation ($\gamma\gamma$) fails to describe both the scale and shape of the data, including radiation brings the prediction in fair agreement with the data. In particular, radiation makes the P_T and $\Delta\phi$ distributions harder because of the presence of at least one hard jet in the final state of events in which one photon originates from radiation. The mass distributions show a

reasonable agreement with the data for all predictions above the peak at 30 GeV/ c^2 , particularly in the region 80 GeV/ $c^2 < M < 150$ GeV/ c^2 relevant to searches for the Higgs boson [1]. However, all predictions underestimate the data around and below the peak. In the P_T spectrum all predictions underestimate the data in the region between 20 and 50 GeV/ c , a feature also observed in the earlier measurements [9,20]. For $P_T < 20$ GeV/ c , where soft-gluon resummation is most important, only the RESBOS prediction describes the data. Discrepancies between the data and theory are most prominent in the comparison of the measured and predicted distributions of $\Delta\phi$. In this case all three predictions fail to describe the data across the whole spectrum. Approaching $\Delta\phi = \pi$, where soft-gluon processes are expected to manifest, the RESBOS prediction agrees better with the data. In the range 1.4 rad $< \Delta\phi < 2.2$ rad, only the PYTHIA prediction describes the data and remains closest to the data down to 1 rad. In the low $\Delta\phi$ tail, which corresponds to the region of low M (< 50 GeV/ c^2), all three predictions are lower than the data, although the DIPHOX prediction, by explicitly including nonperturbative fragmentation, lies closer to the data for $\Delta\phi < 1$ rad.

In summary, the diphoton production cross section, differential in kinematic variables sensitive to the reaction mechanism, is measured by using data corresponding to an integrated luminosity of 5.36 fb $^{-1}$ collected with the CDF II detector. The high statistics of the measured sample allows for a higher precision scan over a much more extended phase space than previous measurements. The overall systematic uncertainty is limited to about 30%. The results of the measurement are compared with three state-of-the-art calculations, applying complementary techniques in describing the reaction. All three calculations, within their known limitations, reproduce the main features of the data, but none of them describes all aspects of the data. The inclusion of photon radiation in the initial and final states significantly improves the PYTHIA parton shower calculation (see the left-hand panels in Fig. 1), which is suitable for background simulations in searches for a low mass Higgs boson and new phenomena.

We thank the Fermilab staff and the technical staffs of the participating institutions for their vital contributions. We also thank P. Nadolsky, C.-P. Yuan, Z. Li, J.-P. Guillet, C. Schmidt, and S. Mrenna for their valuable help in the theoretical calculations. This work was supported by the U.S. Department of Energy and National Science Foundation; the Italian Istituto Nazionale di Fisica Nucleare; the Ministry of Education, Culture, Sports, Science and Technology of Japan; the Natural Sciences and Engineering Research Council of Canada; the National Science Council of the Republic of China; the Swiss National Science Foundation; the A. P. Sloan Foundation; the Bundesministerium für Bildung und Forschung, Germany; the Korean World Class University Program,

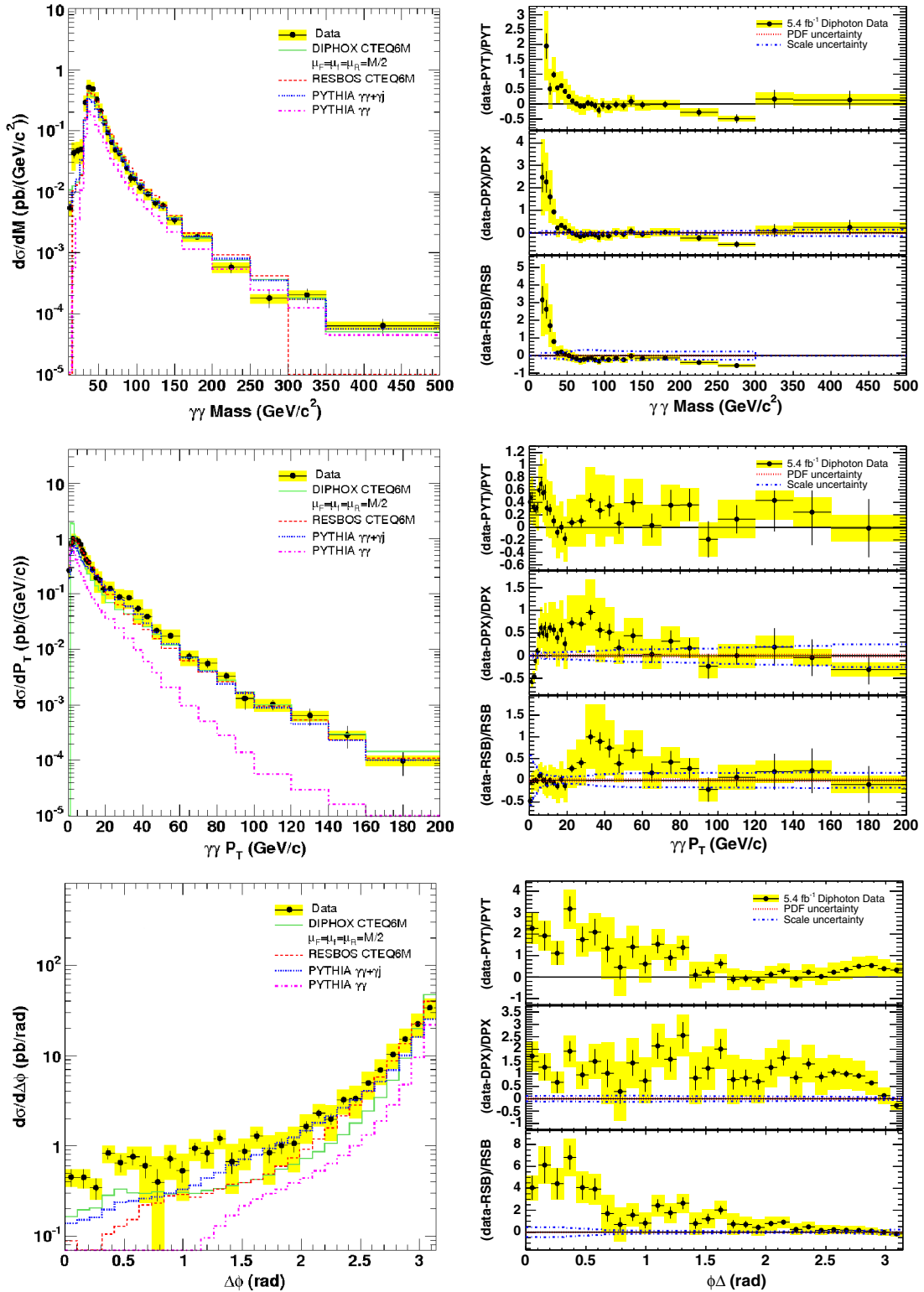


FIG. 1 (color online). The measured differential cross sections compared with three theoretical predictions discussed in the text. The left windows show the absolute comparisons, and the right windows show the fractional deviations of the data from the theoretical predictions. Fractional deviations for PYTHIA refer to the $\gamma\gamma + \gamma j$ calculation. Note that the vertical axis scales differ between fractional deviation plots. The comparisons are made as functions of the diphoton mass (top), transverse momentum (middle), and azimuthal angle difference (bottom). The shaded area around the data points indicates the total systematic uncertainty of the measurement.

the National Research Foundation of Korea; the Science and Technology Facilities Council and the Royal Society, United Kingdom; the Institut National de Physique Nucleaire et Physique des Particules/CNRS; the Russian Foundation for Basic Research; the Ministerio de Ciencia e Innovación, and Programa Consolider-Ingenio 2010, Spain; the Slovak R&D Agency; the Academy of Finland; and the Australian Research Council.

^aDeceased.

^bVisitor from University of Massachusetts Amherst, Amherst, MA 01003, USA.

^cVisitor from Istituto Nazionale di Fisica Nucleare, Sezione di Cagliari, 09042 Monserrato (Cagliari), Italy.

^dVisitor from University of California Irvine, Irvine, CA 92697, USA.

^eVisitor from University of California Santa Barbara, Santa Barbara, CA 93106, USA.

^fVisitor from University of California Santa Cruz, Santa Cruz, CA 95064, USA.

^gVisitor from CERN, CH-1211 Geneva, Switzerland.

^hVisitor from Cornell University, Ithaca, NY 14853, USA.

ⁱVisitor from University of Cyprus, Nicosia CY-1678, Cyprus.

^jVisitor from University College Dublin, Dublin 4, Ireland.

^kVisitor from University of Fukui, Fukui City, Fukui Prefecture, Japan 910-0017.

^lVisitor from Universidad Iberoamericana, Mexico D.F., Mexico.

^mVisitor from Iowa State University, Ames, IA 50011, USA.

ⁿVisitor from University of Iowa, Iowa City, IA 52242, USA.

^oVisitor from Kansas State University, Manhattan, KS 66506, USA.

^pVisitor from University of Manchester, Manchester M13 9PL, United Kingdom.

^qVisitor from Queen Mary, University of London, London, E1 4NS, United Kingdom.

^rVisitor from Muons, Inc., Batavia, IL 60510, USA.

^sVisitor from Nagasaki Institute of Applied Science, Nagasaki, Japan.

^tVisitor from National Research Nuclear University, Moscow, Russia.

^uVisitor from University of Notre Dame, Notre Dame, IN 46556, USA.

^vVisitor from Universidad de Oviedo, E-33007 Oviedo, Spain.

^wVisitor from Texas Tech University, Lubbock, TX 79609, USA.

^xVisitor from Universidad Tecnica Federico Santa Maria, 110v Valparaiso, Chile.

^yVisitor from Yarmouk University, Irbid 211-63, Jordan.

^zOn leave from J. Stefan Institute, Ljubljana, Slovenia.

[1] T. Aaltonen *et al.* (CDF Collaboration), *Phys. Rev. Lett.* **103**, 061803 (2009); V.M. Abazov *et al.* (D0

Collaboration), *Phys. Rev. Lett.* **102**, 231801 (2009); G. Aad *et al.* (ATLAS Collaboration), arXiv:0901.0512; G. L. Bayatian *et al.* (CMS Collaboration), *J. Phys. G* **34**, 995 (2007).

[2] S. Mrenna and J. Willis, *Phys. Rev. D* **63**, 015006 (2000), and references therein.

[3] M. C. Kumar, P. Mathews, V. Ravindran, and A. Tripathi, *Phys. Lett. B* **672**, 45 (2009).

[4] T. Aaltonen *et al.* (CDF Collaboration), *Phys. Rev. D* **83**, 011102 (2011).

[5] G. F. Giudice and R. Rattazzi, *Phys. Rep.* **322**, 419 (1999).

[6] E. Bonvin *et al.* (WA70 Collaboration), *Z. Phys. C* **41**, 591 (1989); *Phys. Lett. B* **236**, 523 (1990).

[7] C. Albajar *et al.* (UA1 Collaboration), *Phys. Lett. B* **209**, 385 (1988).

[8] J. Alitti *et al.* (UA2 Collaboration), *Phys. Lett. B* **288**, 386 (1992).

[9] F. Abe *et al.* (CDF Collaboration), *Phys. Rev. Lett.* **70**, 2232 (1993); D. Acosta *et al.* (CDF Collaboration), *Phys. Rev. Lett.* **95**, 022003 (2005).

[10] V.M. Abazov *et al.* (D0 Collaboration), *Phys. Lett. B* **690**, 108 (2010).

[11] CDF II Collaboration, FERMILAB-PUB-96/90-E, 1996; see also A. Sill *et al.*, *Nucl. Instrum. Methods Phys. Res., Sect. A* **447**, 1 (2000); T. Affolder *et al.*, *Nucl. Instrum. Methods Phys. Res., Sect. A* **526**, 249 (2004) for the spectrometer; L. Balka *et al.*, *Nucl. Instrum. Methods Phys. Res., Sect. A* **267**, 272 (1988); S. Bertolucci *et al.*, *Nucl. Instrum. Methods Phys. Res., Sect. A* **267**, 301 (1988) for the central calorimeters.

[12] T. Aaltonen *et al.*, arXiv:0910.5170v1 [Phys. Rev. D (to be published)].

[13] The calorimeter isolation is defined as the difference of the transverse energy $E_T = E \sin\theta$ in the isolation cone minus the transverse energy in the tower cluster of the photon. The isolation cone is defined to have a radius $R = \sqrt{(\Delta\eta)^2 + (\Delta\phi)^2} = 0.4$ around the axis of the shower profile, where $\eta = -\ln[\tan(\theta/2)]$ is the pseudorapidity, θ is the polar angle, and ϕ is the azimuth in the coordinate system of the laboratory with polar axis along the colliding beams and origin at the center of the detector. The isolation cut implies that the angular separation of the two photons is $\Delta R \geq 0.4$.

[14] The track isolation is defined as the scalar sum of the transverse momenta $p_T = |\vec{p}| \sin\theta$ of all tracks originating from the primary vertex of the event and lying within the photon reconstruction cone.

[15] T. Sjöstrand, P. Eden, C. Friberg, L. Lombard, G. Miu, S. Mrenna, and E. Norrbin, *Comput. Phys. Commun.* **135**, 238 (2001); the version of PYTHIA used here is 6.2.16.

[16] E. Gerchtein and M. Paulini, CHEP-2003-TUMT005, arXiv:physics/0306031; the version of GEANT used for the detector simulation is 3.21; see the CERN Program Library Long Writeup W5013.

[17] The complementary cone is defined by rotating the photon reconstruction cone by an azimuthal angle of 90° about the beam axis, keeping the polar angle fixed.

[18] S. Klimenko, J. Konigsberg, and T.M. Liss, FERMILAB Report No. FERMILAB-FN-0741, 2003.

[19] W.-M. Yao *et al.* (Particle Data Group), *J. Phys. G* **33**, 31 (2006).

- [20] T. Binoth, J. P. Guillet, E. Pilon, and M. Werlen, *Eur. Phys. J. C* **16**, 311 (2000); *Phys. Rev. D* **63**, 114016 (2001).
- [21] L. Bourhis, M. Fontannaz, and J. P. Guillet, *Eur. Phys. J. C* **2**, 529 (1998).
- [22] C. Balazs, E. L. Berger, P. Nadolsky, and C.-P. Yuan, *Phys. Lett. B* **637**, 235 (2006); *Phys. Rev. D* **76**, 013009 (2007); P. Nadolsky, C. Balazs, E. L. Berger, and C.-P. Yuan, *Phys. Rev. D* **76**, 013008 (2007).
- [23] J. Pumplin, D.R. Stump, J. Huston, H.L. Lai, P. Nadolsky, and W.K. Tung, *J. High Energy Phys.* **07** (2002) 012.